

AGRICULTURE DROUGHT AND FOREST FIRE MONITORING IN CHONGQING CITY WITH MODIS AND METEOROLOGICAL OBSERVATIONS*

HONGRUI ZHAO^a ZHONGSHI TANG^a, BIN YANG^b AND MING ZHAO^a

^a 3S Centre, Tsinghua University, Beijing, 100084, China

^b College of Resources and Safety Engineering, China University of Mining and Technology (Beijing), Beijing, 100083, China

KEY WORDS: Forest Fire, Remote Sensing, Monitoring, Agriculture drought

ABSTRACT:

In 2006, Chongqing suffered from agriculture drought that happens once a hundred years, and forest fire was caused at the same time. In order to provide accurate and timely data to Chongqing Government for their decision making, we took MODIS (Moderate Resolution Imaging Spectroradiometer) as remote sensing data resource, and meteorological observations as another important data. To simplify the problem and make the solution more practical, agriculture drought is expressed with soil moisture index (SI) which is generated from LST(land surface temperature) and NDVI. For LST retrieval, a fast statistical model based on meteorological observations is deduced. Forest fire monitoring is accomplished with a comprehensive threshold method, in which reflective bands, middle infrared bands and thermal infrared bands are used together.

1. INTRODUCTION

Chongqing city is one of the most important cities in the Southwestern of China. With fast developing economy and frequent human being activities, its ecological environment is becoming weak and disasters occur frequently in this area. In 2006, Chongqing suffered from agriculture drought that happens once a hundred year, and forest fire was caused at the same time. In order to provide accurate and timely data to Chongqing Government for their decision making, we took MODIS (Moderate Resolution Imaging Spectroradiometer) as remote sensing data resource, and meteorological observations as another important data. To simplify the problem and make the solution more practical, a scheme that combines remote sensing data with meteorological data is proposed for monitoring agriculture drought and forest fire in Chongqing.

This paper is divided into three parts. Part I is about land surface temperature (LST) retrieval, which is one of the most important parameter in environment remote sensing. It is the foundation of both agriculture drought and forest fire monitoring. A LST retrieval physical model is analyzed. Though the retrieved LST meets a higher precision, however, the method is not as efficient as needed. A fast statistical model based on meteorological observations is deduced.

Following LST retrieval, part II describes agriculture drought monitoring. Agriculture drought is regarded as a complex natural event and one of the most damaging environmental phenomena. Combining with the operational meteorological observations, a soil moisture index (SI) was presented. SI was generated according to NDVI and LST for operational production.

However, drought monitoring with remote sensing is difficult, since drought is affected by many factors and always lasting for longer time. With the operational meteorological observations

included, we try to deduce a simple method which can be used in daily drought monitoring in Chongqing city.

Based on the monitoring result, the character of agriculture drought in Chongqing is analyzed at the end of part II.

Part III discusses about forest fire remote sensing monitoring. Forest fire broke out frequently in summer of 2006 in Chongqing city. It resulted from the lack of rain and a continuous hot weather which was rare in the century but happened in summer 2006 in Chongqing. As a result, forest fire occurred 6 times a day in average from August 1st to 13th in Chongqing city.

For higher temperature forest fire points, channel 7 of MODIS is mainly used and the fire points are detected in a more direct way.

Non-high temperature forest fire points are classified into 3 types. They are the points before firing, the fired points and the firing points with a smaller area than that of the image spatial resolution. A comprehensive threshold method was proposed with reflective bands, middle infrared bands and thermal infrared bands used together. Reflective bands were used to eliminate pseudo-fire points that resulted from city hot island. Middle infrared bands and thermal infrared bands were used to detect 3 types of non-high temperature forest fire points. The forest fire monitoring result is analyzed at the end of this part.

In comparison with the soil moisture observation, the operational meteorological data, the remote sensing inversion result of soil moisture index is coherent with the ground truth. However, our research reveals that the drought monitoring model will be more practical along with accumulation of drought monitoring data including remote sensing data and meteorological observations. In fact, both the inversion model

-
- Supported by the National Natural Science Foundation of China (Grant No. 40771135)
 - Corresponding Author * HONGRUI ZHAO. Telephone: 8610-62794967; Email: zhr@tsinghua.edu.cn

and meteorological observations are prior knowledge for renew SI model.

Fire points are identified according to its temperature that is much higher than the background. Generally, the temperature of forest fire is around 600K. However, some points do not reveal such a higher temperature in remote sensing than that of in the reality because of the spatial resolution of the image. So we divided forest fire points into two types, which were higher temperature forest fire points and non-high temperature forest fire points. They were treated in different ways with different channels of MODIS.

2. LST RETRIEVALTITLE

Land surface temperature (LST) retrieval, which is one of the important parameter in environment remote sensing, is also a most difficult one in the field of remote sensing. Many scholars worked on this subject and achieved many researches results, such as thermal radiative transfer equation method, mono-window algorithm, split-window algorithm, and multi-channels algorithm. (Price J C, 1984; Becker F, 1987; Cooper D I, 1989; Becker F, 1990; Sobrino J A, 1991; Prata A J, 1993; Wan Z, 1997; Li Zhaoliang, 1999; Shunlin Liang, 2001; Ma X-L, 2000)

Generally, these models are divided into two categories, physical models and statistical models. Our experiments in Chongqing show that the physical model has a better performance. Ma's physical model is used in our experiments duo to its good LST retrieval performance (Ma X-L, 2000). It is an integrated inversion algorithm with land surface and atmosphere parameters retrieved together.

For a cloud-free atmosphere under local thermodynamic equilibrium the RTE (Radiative Transfer Equation) in the thermal infrared region may be expressed as below. (Ma X-L, 2000)

$$R(v_j, \mu) = \underbrace{B(v_j, t_s) \varepsilon(v_j, \mu) \tau(v_j, \mu, p_s)}_1 + \underbrace{R_a(v_j, \mu)}_2 \quad (2-1)$$

$$+ \underbrace{\int_0^{2\pi} \int_0^1 \mu' f_r(\mu; -\mu', \phi') R_d(v_j, \mu, -\mu', \phi') d\mu' d\phi'}_3$$

$$+ \underbrace{\tau^*(v_j, \mu, -\mu_0, 0) E_0(v_j) f_r(\mu; -\mu', \phi')}_4$$

In this formula, $R(v_j, \mu)$ is the mean spectral radiance measured in a band whose mean effective wave number is v_j and the cosine of local zenith angle θ is μ , $B(v_j, t_s)$ is the Planck function of the surface skin temperature t_s , $\varepsilon(v_j, \mu)$ is the effective surface emissivity, and $\tau(v_j, \mu, p_s)$ is the transmittance from the surface pressure level p_s to the top of the atmosphere along the observation angle θ . The first term of Eq. (1) represents surface emission to space (less atmospheric absorption). $R_a(v_j, \mu)$ is the upwelling radiance contributed from atmosphere to space.

$R_d(v_j, \mu, -\mu', \phi')$ denotes the atmospheric downwelling emissive radiance being reflected by the surface upward to space; its incident direction is represented by $-\mu'$ and ϕ' (where the minus sign indicates that direction is always downward). (Ma X-L, 2000)

Though we have improved Ma's model and got a higher precision of the retrieved target parameter LST, the improved inversion method is not as efficient as needed. A significant disadvantage is its large quantity of calculation, which makes the method too complex to be widely used in operational application. Furthermore, Chongqing city has its own characteristics, mountainous terrain and cloudy climate. Ma's model may not be applicable in such a reality, so it is better to develop a new linear statistical model as simple as it could.

On the base of an intensive comprehension of the physical model, we deduced a linear exponential expression with both MODIS and observation data in July and August, 2006.

$$LST = 2.7932(BT_{31} - BT_{32}) - 0.1781BT_{31} + 354.3806 \quad (2-2)$$

where BT_i $i=31,32$ are the brightness temperatures of MODIS bands 31 and 32.

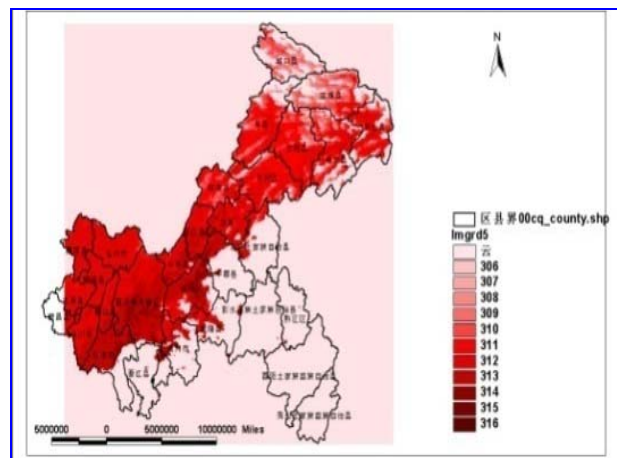


Figure 1-1 LST retrieval results on August 7th, 2006

Compared with the meteorological data through July and August, 2006, LST retrieved with the linear model matched quite well with the observation data in Fengjie, Youyang, Fuling, Liangping, Shapingba, and Wanzhou. Figure 1-1 is the LST inversion result on August 7th, 2006 (The white area is covered with cloud).

However, it is better to combine the physical model and statistical model together, so as to get a better retrieval precision of the target parameter in a practical way. We are working on this purpose now, and the result will be presented soon.

3. RESEARCH DROUGHT MONITORING IN CHONGQING WITH REMOTE SENSING

3.1 The Status of Drought Monitoring with Remote Sensing

The agriculture drought indicators in China are generally divided into three categories: precipitation index, soil moisture indicator, water balance indicator. Soil moisture is one of the important drought indicators. It is the major parameter in climate, ecological, agricultural areas. Drought often happens in large areas and lasts for a period of time, it is easy to cause serious losses. With the development of remote sensing technology, multiphase, multi-spectral of remote sensing data may provide information related with surface soil moisture and. It can be used to evaluate soil water conditions and monitor agriculture drought.

NOAA/AVHRR (Kogan.F, 1997), Landsat TM were often used for drought monitoring. Now, MODIS plays an important role in agriculture drought monitoring. The following are the major methods.

- i) Thermal inertia approach. It usually applies to bare land or low vegetation coverage area for remote sensing drought monitoring.
- ii) Vegetation supply water index. This method is particularly suitable for vegetation coverage area or the abundance of vegetation in better.
- iii) Energy index model. It is more suitable for soil moisture monitoring.
- iv) Temperature vegetation drought index. This method has been used in regional drought monitoring and has achieved very good results. And so is water stress index (WDI).

3.2 Soil Moisture Index

Soil moisture is an important index in Chongqing agriculture drought monitoring. There are 170 soil moisture (SI) observation points in Chongqing city. SI is observed from March to October on every 3rd and 8th. The data used in our experiment was August 4th to 9th 2006, which was supported by the Chongqing Municipal Climate Center. Drought degrees are as follows: Soil relative humidity $\leq 30\%$: special drought; 30 to 40 percent: heavy drought; 40 to 50 percent: moderate drought; 50 to 60 percent: Light drought; 60 to 90 percent: suitable or basic suitable; $> 90\%$: too wet.

3.2.1 The Necessity of Researching Soil Moisture Index

Since a MODIS station has been constructed in Chongqing city. It is convenient to use MODIS as a remote sensing data resource in agriculture drought monitoring in Chongqing. The greatest advantage of remote sensing drought monitoring is its real-time, fast, and objective. The greatest disadvantage is lack of ground verification. So it is necessary to combine weather observation, the ground truth observation and remote sensing information together to fulfil accurate soil moisture monitoring.

3.2.2 Affecting Factors of Soil Moisture

The major factor of agricultural drought monitoring is the crop water stress. So, the growth of crops and temperature (surface temperature, including the canopy temperature) are important indicators. The expression of soil moisture function can be expressed as the following function:

$$SMI = f(NDVI, LST) \quad (3-1)$$

Vegetation index is used by the most researchers, and it is the factor in operational work. Many scholars research a variety of vegetation indexes. After analyzing and comparing the vegetation indexes, the test with MODIS data from July to August in Chongqing city shows that there is no saturation in normalized difference vegetation index (NDVI), so we decide to use NDVI as vegetation index.

3.3 Soil Moisture Retrieval Practice in Chongqing Summer of 2006

Soil moisture retrieval formula is deduced by regression of remote sensing data and ground observation data:

$$SMI = 0.856 \times \frac{NDVI \times 300}{LST} - 0.0189 \quad (3-2)$$

Where LST is land surface temperature (K). NDVI is obtained by reflectivity of MODIS band 1 and band 2.

$$NDVI = \frac{r_2 - r_1}{r_2 + r_1} \quad (3-3)$$

Where r_1, r_2 are reflectivity of MODIS band 1 and band 2.

Figure 3-1 is Chongqing NDVI map on August 7th, 2006, without removing cloud area. The cloud areas were removed in soil moisture calculation.

The results are shown in Figure 3-2 and Figure 3-3:

Figure 3-2 is the retrieval soil moisture map. Each pixel corresponds quantitative soil moisture. The region with value of 0 is cloud area and not involved in the calculation of moisture.

Figure 3-3 is the classification of soil moisture map basing on Figure 3-2. Regions 1, 2, 3 and 4 denote special heavy drought, heavy drought, moderate drought and slight drought. In our study the soil moisture only referred to the moisture of 0-10cm below the land surface.

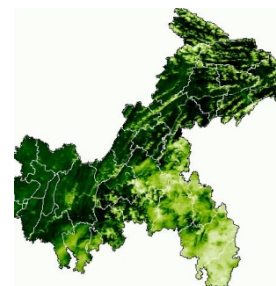


Figure 3-1 Chongqing NDVI on August 7th, 2006

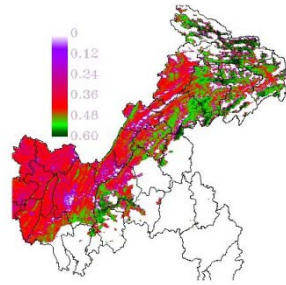


Figure 3-2 Chongqing soil moisture on August 7th, 2006

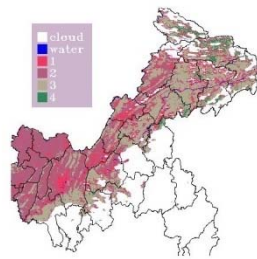


Figure 3-3 Chongqing soil moisture on August 7th, 2006

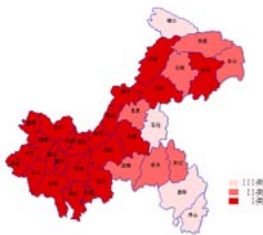


Figure 3-4 Meteorological Observation of Chongqing Drought in Summer of 2006 (July 21st—August 10th)

Figure 3-4 shows the drought distribution observed by Chongqing Municipality Climate Centre.

Comparing the monitoring results from Chongqing Climate Centre with remote sensing retrieval results, we find that they are basically consistent. However, remote sensing retrieval result is more objective due to its regional characteristic. It can be seen that political borders of counties are obvious in that of that meteorological observation data, because the meteorological observations are point data. Therefore, quantitative remote sensing retrieval soil moisture is more macro, objective, real-time in monitoring the actual local drought status.

4. FOREST FIRE MONITORING IN CHONGQING

4.1 Research Methods

According to Wilhelm Wien's Displacement Law (Price J C, 1983), MODIS bands 20, 21, 22 and 23 are designed for monitoring forest fire, which temperature is about 600 K and atmospheric window (8-14 μm) bands 31 and 32 are used to retrieval land surface temperature which temperature is about 300 K. For the forest fire with smaller size, especially when

forest fire area is smaller than that of a pixel, band 31 and band 32 have important significance for the fire points monitoring. Furthermore, Channel 7 of MODIS has 500m spatial resolution. Our experiment showed that it is sensitive to high temperature, especially 600 ~ 1000K, though this channel has often been neglected in monitoring forest fires. We believe band 7 will greatly helpful for forest fire identification.

Figure 4-1 and Figure 4-2 are brightness temperature of band 21 and band 31 respectively.

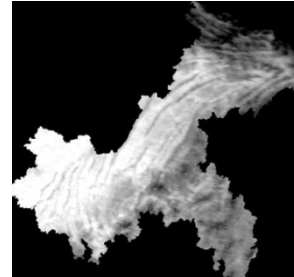


Figure 4-3 Brightness temperature of band 21 on August 11th

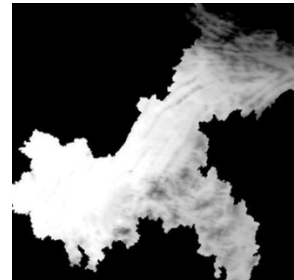


Figure 4-4 Brightness temperature of band 31 on August 11th

4.2 The Process and Results

4.2.1 Direct Method for Detecting High Temperature Fire Points

We use band 7 to detect high temperature fire points. Figure 4-3 is the composite image of MODIS bands 7, 4 and 3. Figure 4-4 is the enlarged one. The arrows point to two fire points. The left one is a high temperature open fire point. The right one is suspected a hidden fire point. According to reality information, at 12:00 on August 11th, Bishan county, Aokang Industrial Park, Tiger hill occurred forest fire (fire should be 1). At 11:30 on August 11th, Shapingba, Zengjia county occurred forest fire (fire should be 2). And this image's acquisition time was August 11th, MODIS (TERRA) crossing at local time 10:30, it was the very likely reason why fire point 2 has no smoke plume. In addition, some fires can also be found in Banan.

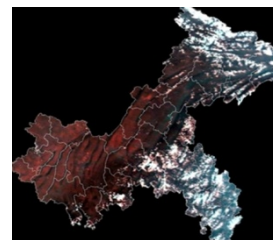


Figure 4-3 RGB composite image of bands 7, 4, 3

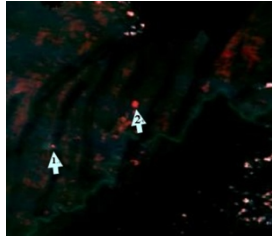


Figure 4-4 Local fire points on August 11th

Figure 4-5 is scatter plot of brightness temperature of band 22 and band 23, the abscissa is band 22; Figure 4-6 is scatter plot of the brightness temperature of band 20 and band 21, and the abscissa is band 20. We can clearly see abnormal points from the plot. Abnormal points are far away from points group. These abnormal points are most likely due to the saturation of bands 20, 22. The uncertainty data is in band 22 which can be got from HDF document. Many researchers use band 21 only because of its unsaturation, and abnormal data in band 20 and band 22 was often discarded. Our experiment shows that it is an efficient way to use these "abnormal" data combining with band 7 to detect high temperature fires.

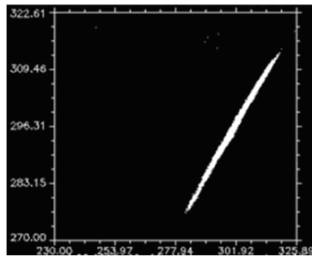


Figure 4-5 Scatter plot of bands 22, 23

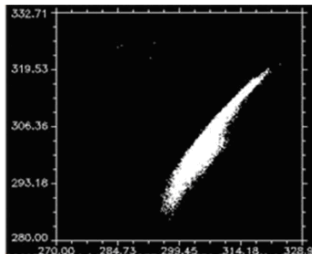


Figure 4-6 Scatter plot of bands 20, 21

4.2.2 Non-high Temperature Fires Judged with Comprehensive Threshold Criterion

Non-high temperature fires include three major types: i) before the fire occurred with the temperature lower than ignition temperature; ii) after fire occurred, the temperature had fallen, but higher than normal temperature; iii) The fire point is at high temperature, but the firing area is smaller than that of a pixel. There are many difficulties and uncertainties in non-high temperature fire monitoring, particularly the third category of non-high temperature fires. Therefore, many researchers define the fire point that burning area is larger or equal to one pixel size. With non-high temperature fires complex situations considered, a comprehensive threshold criterion is used in our work. We combine visible, near-infrared, mid-infrared and thermal infrared bands together to get an integrated application. First, visible and near infrared bands (MODIS bands 1, 2) are

used to generate NDVI. NDVI has two roles: i) The fire area where NDVI is less than 0.3 generally reveals combustibles; ii) Generally, there are unburned vegetations with higher NDVI around the fire place. The above two are used together to judge forest fire points. At the same time, according to the characteristics of the forest fire, we use the differences of brightness temperatures between band 21 and band 31 to judge fires. The comprehensive threshold is:

$$\begin{cases} NDVI \leq 0.3 \\ BT_{21} - BT_{31} \geq 15 \\ BT_{21} \geq 315 \\ BT_{31} \geq aver(BT_{31}) \end{cases} \quad (4-1)$$

Where BT_{21} is the brightness temperature of band 21, BT_{31} is the brightness temperature of band 31, $aver(BT_{31})$ is the average non-cloudy pixel's brightness temperatures of band 31.

Suspected fire points are generated with the comprehensive threshold, a second judgment is followed which purpose is to identify whether the background pixels are forest. It can be achieved with NDVI. Figure 4-7 is the result of using comprehensive threshold on August 11th, 2006.

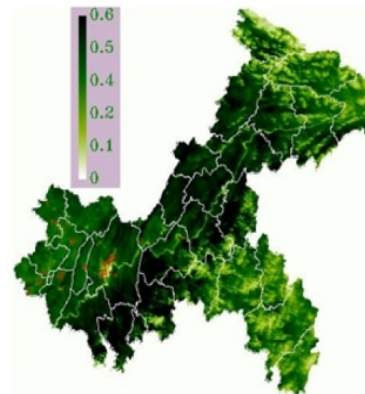


Figure 4-7 The suspected fires points generated by threshold criterion on NDVI of August 11th, 2006 (red areas were suspected fires, high temperature points in low NDVI were suspected as urban heat islands)

In Figure 4-7, the further judgment is based on background pixels. If we can integrate land-use data, the accuracy will be improved. We can exclude most places with high temperature result from urban heat island. Other high temperature points may be fire points or ground facilities (further judgments with ground truth are needed).

In order to make a further test, we extracted and analysed the data on August 8th and August 30th, 2006. Figure 4-8, figure 4-9, figure 4-10 and figure 4-11 were the results.

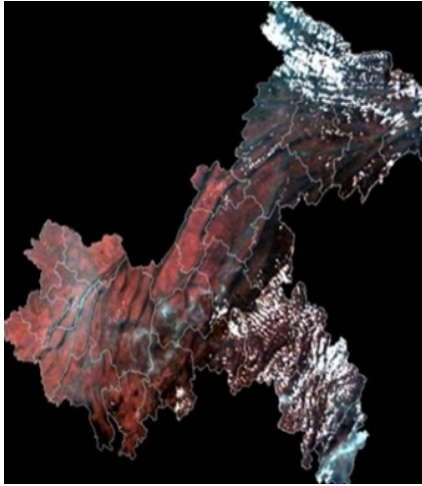


Figure 4-5 RGB composite image of band 7, 4, 3 on August 8th



Figure 4-6 Suspected fire points on NDVI image of August 8th

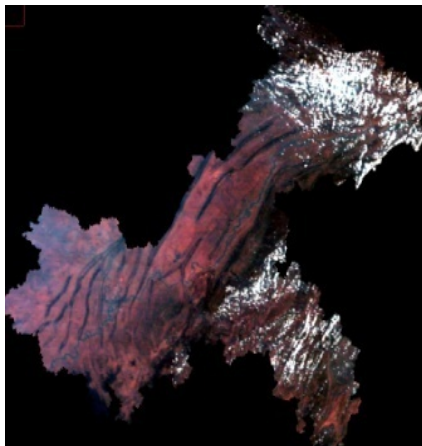


Figure 4-7 RGB composite image of band 7, 4, 3 on August 30th



Figure 4-8 Suspected fire points on NDVI image of August 30th

Though some detected high temperature points were not forest fire points, however, the real forest fire points have been detected with our method. The result shows that it is a good choice to monitor forest fires with MODIS.

5. CONCLUSIONS AND DISCUSSIONS

In our experiment, LST is retrieved with a statistical model. Though the accuracy of LST is to be improved, the method is an effective in operation work. However, as time passed, the statistical model will be refined with more prior knowledge used in the regression. So does the SI model.

Since the physical model for LST retrieval has a better precision. Our next study will aims on combining the physical model and the statistical model together so as to get a precise and effective inversion way.

Though channel 7 was not designed for forest fire detection, higher temperature forest fire points show higher reflectivity in this channel. Combined with channel 7 and 4 middle infrared bands (band 20-23) that designed for forest fire, higher temperature forest fire points are detected with a higher precision.

It can be concluded that MODIS is an ideal data source in agriculture drought monitoring and forest fire monitoring. Furthermore, in order to get more objective information, it is a better way to combine remote sensing data and meteorologic operational data together.

REFERENCES

- Becker F, Li Zhaoliang, 1990. Towards a Local SplitWindow Method Over land surface. *Int. J. Remote Sens.*, 3: 369-393
- Becker F, 1987. The impact of spectral emissivity on the measurement of land surface temperature from a satellite. *Int. J. Remote Sens.*, 8 (10): 1509-1522.
- CooperD I, Asrar G, 1989. Evaluating atmospheric correction models for retrieving surface temperatures from the AVHRR over a tall grass prairie. *Remote Sens. Environ.*, 27: 93-102.

Holbo H. R. J. C. Luvall, 1989. Modeling surface temperature distributions in forest landscapes, *Remote Sens. Environ.*, (27):11-24.

Kogan, F., 1997. Global drought watch from space, *Bull. Am. Meteorol. Soc.*, 78: 621-636.

Li Zhaoliang, Becker F, StollM P. Evaluation of six methods for extracting relative emissivity spectra from thermal infrared images. *Remote Sensing of Environment*, 1999, 69: 197 - 214.

Ma X. L., Wan Z. M., Moeller C. C., et al., Retrieval of geophysical parameters from moderate resolution imaging spectroradiometer thermal infrared data: evaluation of a two-step physical algorithm, *Appl. Opt.* 2000, 39: 3537~3550.

Prata A J, 1993. Land surface temperature derived from the Advanced Very High Radiometer and the Along - Track scanning Radiometer 1. *Geophys. Res.*, 98 (D9) : 16689-16702.

Price J C, 1983. Estimating surface temperature from satellite thermal infrared data—A simple formulation for the atmospheric effect. *Remote Sens Environ.*, (13):353-361.

Price J C, 1984. Land surface temperature measurements from the splitwindow channels of the NOAA 7 /AVHRR. *Geophys. Res.*, 89: 7231-7237.

Shunlin Liang, 2001. An optimization algorithm for separating land surface temperature and emissivity from multispectral thermal infrared imagery. *IEEE Transaction on Geosciences and Remote Sensing*, 39 (2) : 264-274.

Sobrino J A, Coll C, CasellesV, 1991. Atmospheric corrections for land surface temperature using AVHRR channel 4 and 5. *Remote Sensing Environ.*, 38 (1) : 19-34.

Wan Z, Li Zhaoliang, 1997. A physics-based algorithm for retrieving land surface emissivity and temperature from EOS/MODIS data. *IEEE Transaction on Geosciences and Remote Sensing*, 35 (4) : 980-996.

